Journal of Membrane Science Letters 2 (2022) 100010

Contents lists available at ScienceDirect

Journal of Membrane Science Letters

journal homepage: www.elsevier.com/locate/memlet

New parametrization method for salt permeability of reverse osmosis desalination membranes

P.M. Biesheuvel [a,*], J.E. Dykstra [b], S. Porada [a], M. Elimelech [c]

[a] Wetsus, European Centre of Excellence for Sustainable Water Technology, The Netherlands
[b] Environmental Technology, Wageningen University, The Netherlands
[c] Department of Chemical and Environmental Engineering, Yale University, USA

A B S T R A C T

Reverse osmosis (RO) is the most important membrane technology for the desalination of water. Measured water and salt fluxes are traditionally analyzed in the context of the solution-diffusion (SD) model which leads to a water permeability, A, and a salt permeability, B. However, this parametrization of the salt flux is not correct for water desalination by RO membranes, because these membranes show markedly different retentions for different feed salt concentrations, a classical observation in the literature, and this effect is not captured by the SD model. Thus, the traditional salt permeability B is not an intrinsic property of these membranes. We present a new analysis for desalination of a 1:1 salt, which follows from a transport theory that is based on the assumption that coions are strongly excluded from the membrane, and we demonstrate that it accurately describes a large dataset of salt retention by an RO membrane as function of pressure and feed salt concentration. This analysis leads to unique values of the water and salt permeabilities, A and B'', not dependent on salt concentration or permeate water flux. Because we now have an improved parametrization, we can more accurately compare different membranes or study in more detail how membrane performance depends on conditions such as salt type and temperature. The new equation can provide guidance for the design of high-performance desalination membranes and for process modeling of desalination systems.

Statement of novelty: Reverse osmosis is the most important membrane-based water technology. Membranes are often characterized by two permeabilities, A and B, and in comparison and simulation studies it is often assumed they are intrinsic parameters of the membrane. However, it is also known in literature that B is not such an intrinsic parameter, but the problem is that an alternative intrinsic salt permeability indicator is not yet available. Based on a theoretical derivation, we present a concise new parametrization of the salt permeability of RO membranes that is an intrinsic membrane property. This new parametrization allows for a much better comparison between RO membranes and optimization of membrane performance.

Reverse osmosis (RO) is the leading membrane-based method for water desalination, capable of treating various water sources, from water that is just somewhat too saline for use, into the range of brackish water sources and seawater, as well as water sources with a salinity higher than seawater (Elimelech and Phillip, 2011; Song, 2000; Wang et al., 2021). Experimental testing of RO membranes with simple 1:1 salt solutions (for instance NaCl) leads to useful performance data (Wang et al., 2021). In such experiments, the permeate concentration, c_p, is measured, from which salt retention (also called salt rejection), R_i, is obtained, as well as permeate water flux (also called transmembrane water velocity), v_w, as function of applied hydrostatic pressure (the pressure difference across the membrane), $\Delta P^{h,\infty}$. For low water recovery, The product of permeate concentration and water flux recalculates to a transmembrane salt flux, J_s. From such experiments traditionally two characteristic numbers are derived to parametrize membrane performance, A and B (Riley et al., 1971; Geise et al., 2011; Werber et al., 2016; Chen et al., 2021; et al., Ritt, 2022). These parameters describe water permeability (which ideally is high) and salt permeability (must be low) and are considered to be intrinsic membrane properties. To calculate A and B from data on water and salt fluxes, the solution-diffusion (SD) model is used, which was based on the idea that solvent and salt molecules absorb in the membrane and then diffuse to the other side, and based on this model the two fluxes are renormalized by their respective driving forces, which are the applied pressure difference to calculate A, and the difference in salt concentration across the membrane to calculate B (Lonsdale et al., 1965; Wijmans and Baker, 1995). The diffusion boundary layer (DBL, also called concentration polarization layer, or CP layer) is included in the analysis, to properly calculate membrane-based driving forces.

However, as we will discuss, for salt flux this parametrization is not accurate, which a simple observation already shows, namely that salt retention depends on feed salt concentration (e.g. Song, 2000). Analysis based on the SD model then results in values of B that increase with salt concentration, and this indicates that B is not an intrinsic membrane property (Song, 2000; Wang et al., 2021). This important point was already identified in 1961 when Kedem and Katchalsky wrote “The coefficient [B] does not represent therefore a constant parameter and is expected to change strongly with salt concentration” (Kedem and

* Corresponding author.
E-mail address: maarten.biesheuvel@wetsus.nl (P.M. Biesheuvel).

https://doi.org/10.1016/j.memlet.2021.100010
Received 20 November 2021; Received in revised form 11 December 2021; Accepted 16 December 2021

Katchalsky, 1961). As a consequence, diagrams with (*A*,*B*)-data points of many membranes are not suitable to make an exact comparison between them, unless in all cases identical experimental conditions are used. This dependence of *B* on conditions such as feed salt concentration indicates that the underlying theory is not accurate, and for that reason does not lead to a good parametrization and should not be used for the characterization of RO membrane performance.

We analyze recently published data for desalination by a commercial seawater reverse osmosis (SWRO) membrane (Dupont SW30XLE) (Wang et al., 2021). These data are obtained at different pressures, and for three values of the feed salt concentration, c_f, of a 1:1 salt (NaCl), all for low water recovery. Evaluation of the complete dataset leads to a mass transfer coefficient in the CP layer of $k_{dbl} \sim 100$ L m^{-2} h^{-1} (LMH), which is the value we use in this report. Because of the high salt retention for all data, the simple film model $c_{int} = c_f \exp\left(v_w/k_{dbl}\right)$ can be used for the CP layer, with c_{int} the salt concentration at the DBL/membrane interface, just outside the membrane (e.g., Fig. 11 in Teorell (1956); Eq. (6) in Wijmans et al. (1985)). Following the standard approach, the water permeability, *A*, in unit LMH/bar, is calculated by renormalizing the water flux, v_w, by the pressure difference, $\Delta P^{h,\infty}$, from which the osmotic pressure difference across the membrane, $\Delta\Pi = 2\,RT\left(c_{int} - c_p\right)$, is subtracted. The measured salt flux, J_s, is renormalized by the salt concentration difference, $c_{int} - c_p$, resulting in the salt permeability, *B*, which can be expressed with dimension LMH, i.e., salt flux is assumed to be described by $J_s = B\left(c_{int} - c_p\right)$. A final equation that is implemented is $J_s = v_w\, c_p$, which is valid for an RO-experiment at low water recovery. Combining these equations we obtain $R_i = 1 - \left\{B/\left(v_w + B\right)\right\} e^{v_w/k_{dbl}}$ for retention in the SD model, showing that retention is predicted to be independent of feed (salt) concentration.

The full dataset of R_i versus v_w for three salt concentrations is presented in Fig. 1A together with a fit based on the SD model using $B = 0.25$ LMH. Though a single dataset (at one salinity) can be fitted well, clearly this model is not accurate, because the data show that salt retention depends strongly on feed salt concentration, while according to the SD model this dependency should not exist (Kedem and Freger, 2008). That this model is not accurate is also demonstrated in Fig. 1B where all derived values of *B* are plotted versus *A*. These data for *B* are distributed in a wide range, with over a factor of two difference between low and high bounds (*B* ranging from 0.15 to 0.35 LMH). Clearly, derived *B*-values depend strongly on the salt concentration of the feedwater, whereas the SD-model predicts an absence of this influence, as also concluded in Wang et al. (2021). Water permeability, *A*, can be reasonably well determined as an intrinsic property of the membrane, at $A = 1.65 \pm 0.25$ LMH/bar, see A technical note on data analysis.

To describe water desalination with RO membranes not by the blackbox SD model but by a physics-based mechanistic approach, the solution-friction (SF) model can be used, as recently highlighted in Wang et al. (2021) and earlier reported, for instance in Bowen and Welfoot (2002), Oren and Biesheuvel (2018), Biesheuvel et al. (2020), Kimani et al. (2021). In Wang et al. (2021) a good fit was obtained between calculations with the SF-model and data (the same dataset that is used in the present report), and it was concluded that the standard parametrization to derive a unique *B*-value is not valid. As also shown in Wang et al. (2021), in contrast to the SD-model, when the SF-model is used for desalination, predictions for retention are dependent on feedwater salt concentration, which is in agreement with experimental observations, with better retention for lower feed salt concentration.

We use an analytical model that is based on the SF-approach and that leads to the same conclusion. The derivation is based on the assumption that coions are strongly excluded from the membrane, i.e., are present in the membrane at a very low concentration (Starov and Churaev, 1993). We call this the limit of good coion exclusion (GCE). If coions are at a very low concentration, then they are transported through the membrane as if they are neutral solutes, based on diffusion and advection. If the advective contribution is low (for low permeate water flux, v_w), then they are only transported by molecular diffusion. If that is the case, then in a full numerical calculation, concentration profiles will change linearly across the membrane when indeed other driving forces can be neglected. A similar conclusion, namely that for a charged membrane which strongly excludes coions, at low transmembrane water fluxes, coion transport is mainly due to diffusion, was also arrived at for electrodialysis in Tedesco et al. (2018). In RO with only two ions, the flux of coions equals that of counterions, which equals the salt flux, J_s. In the absence of advection, when only diffusion of coions is of importance, salt flux in steady state is described by $J_s = k_{m,i} K_{f,i} \Delta c_{m,co}$, with Δ describing a difference between a concentration on the upstream side, minus on the downstream side, in both cases just *inside* the membrane; here 'co' refers to the coions, and 'm' refers to concentrations *inside* the membrane. A similar expression is used in the SD model, but then it is applied to neutral solutes, or to the salt as a whole, without distinguishing coions from counterions. In the above equation, $k_{m,i}$ is a transport coefficient of ions in the membrane (unit m/s), given by the ion diffusion coefficient in the membrane divided by membrane thickness, and $K_{f,i}$ is a dimensionless factor with values between 0 and 1 that describes the relative importance of friction of ions with the water relative to that of ions with the membrane matrix, see Wang et al. (2021).

Next we relate coion concentrations just in the membrane to the salt concentration just outside, c_∞. We do that based on a Donnan balance extended with a partitioning coefficient Φ_i (Biesheuvel, 2011; Gamaethiralalage et al., 2021; Sonin, 1976; Wang et al., 2021). This Donnan balance is based on analysis of the Boltzmann equation for each ion, $c_{m,i} = c_\infty\, \Phi_i\, \exp\left(-z_i \phi_D\right)$, where z_i is the ion's valency and ϕ_D the Donnan potential across the solution-membrane interface. If we combine this equation for the cation and anion of a 1:1 salt, and include how in the GCE limit $c_{ct} \sim |X|$, where 'ct' refers to the counterion, then we obtain (Kedem and Katchalsky, 1961)

$$c_{m,co}\,|X| = \left(\Phi_i c_\infty\right)^2 \tag{1}$$

where *X* is the membrane charge density (unit M, defined per volume of aqueous phase inside the membrane; the notation $|X|$ refers to the magnitude of this charge). The partitioning coefficient, Φ_i, is a factor that can include various contributions to the distribution of ions across the solution-membrane interface, see Gamaethiralalage et al. (2021), Wang et al. (2021). Note that this derivation assumes that coions and counterions have the same Φ_i. The salt flux across the membrane is now given by

$$J_s = B'\,RT\left(c_{int}^2 - c_p^2\right) \tag{2}$$

where B' is a modified salt permeability, given by Kedem and Katchalsky (1961)

$$B' = \frac{k_{m,i}\, K_{f,i}\, \Phi_i^2}{RT\,|X|} \tag{3}$$

which has dimension m/Pa.s, that can also be recalculated to LMH/bar. Equation (2) is quite remarkable, because it predicts that the salt flux across the membrane is a function of the salt concentrations on both sides of the membrane, *squared*, in contrast to the linear concentration dependence predicted by the SD model. The quadratic form is arrived at because of the Donnan balance, Eq. (1), that describes how in the GCE limit the coion concentration in the membrane relates to the outside salt concentration to the power two. Equation (9-5) in Kedem and Katchalsky (1961) is Eq. (3) multiplied by c_{int} and assuming $\Phi_i = 1$.

If we implement the expression given above for the CP-layer, and if we assume a high retention, i.e., $c_p \ll c_f$, we can derive an expression for salt retention according to the GCE-model given by

$$R_i = 1 - B'\,RT\,c_f\,v_w^{-1}\,e^{2v_w/k_{dbl}} \tag{4}$$

which predicts that retention not only depends on the permeate water flux, v_w, but also on feed concentration. This is a crucial difference with the SD-model, where the latter dependence is absent.

A more rigorous derivation is based on the extended Nernst-Planck equation for a symmetric 1:1 salt in a charged membrane, including

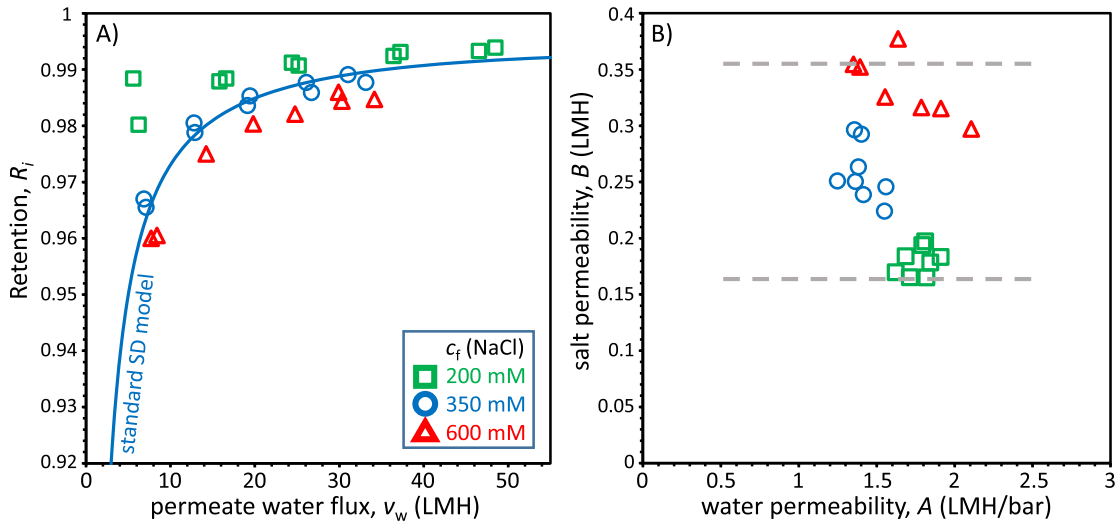

Fig. 1. A) Retention of a 1:1 salt in a SWRO membrane as function of permeate water flux, v_w, and feed salt concentration, c_f. Data from Wang et al. (2021). Fit using SD model with $B = 0.25$ LMH. B) Range of B-values when data are parametrized according to the SD model.

advection, diffusion, and electromigration. In Supplementary Material we provide a full derivation. The resulting expression is (see Eq. (41) in Biesheuvel (2011) and Eq. (32) in Sonin (1976))

$$J_s = 2\, v_w\, |X|^{-1}\, K_{f,i}\, \Phi_i^2\, c_{int}\, c_p\, \frac{\sinh\left(v_w/k_{m,i} + \ln\left(c_{int}/c_p\right)\right)}{\sinh\left(v_w/k_{m,i}\right)} . \tag{5}$$

In addition to the result presented in Biesheuvel (2011) and Sonin (1976), we include here the factors $K_{f,i}$ and Φ_i^2 which are required in the SF-theory and were not in the extended NP-equation and Donnan balance analyzed in Biesheuvel (2011) and Sonin (1976). Now we take an expansion for low water fluxes, and arrive at the elegant result

$$J_s\, \frac{|X|}{K_{f,i}\Phi_i^2} = k_{m,i}\left(c_{int}^2 - c_p^2\right) + v_w\left(c_{int}^2 + c_p^2\right) + \ldots \tag{6}$$

which has a diffusional term and a term linear in water flux v_w. Thus, in the GCE model for low v_w relative to $k_{m,i}$, only the diffusional term is of importance and salt flux does not depend on v_w. However, when v_w becomes of the order of $k_{m,i}$, then advection starts to play a role. If we only consider the contribution of diffusion, we arrive at the earlier result, Eq. (2). At low c_p relative to c_{int} we then arrive at Eq. (4), and it is this equation that from this point onward we use in this letter.

We use this model to describe the aforementioned dataset, and obtain the results presented in Fig. 2, where we use an 'expanded' y-axis compared to Fig. 1, to more clearly show how well theory fits the data. Though the GCE-model fits data reasonably well, similar to the fit using the full SF theory presented in Wang et al. (2021), the fit is not yet fully satisfying, with retention responding too strongly to salt concentration. This deviation is also apparent in Fig. 2B where we summarize the derived values of the modified salt permeability B' according to the GCE-approach, which are obtained from data of the salt flux, by dividing by a factor that involves the concentrations on either side of the membrane, squared, see Eq. (2). Here, similar to results in Fig. 1B, there is quite a large distribution of the derived values for B'. This demonstrates that the model is not accurate enough, because we must have a theory, a parametrization, such that all data of a properly defined salt permeability collapse onto one common value.

The question then is what is wrong in this model, such that effectively the influence of feed salt concentration on retention is overestimated, as can be observed by comparing theory and data in Fig. 2A. It seems unlikely that the problem is directly related to some transport mechanism *inside* the membrane. We make this claim because inside the membrane transport is quite similar for all datasets, with similar values for salt flux and water flux found in all datasets. And for a fixed membrane charge, X, we can expect that in all cases charge compensation by counterions leads to the same counterion concentration in the membrane. One cause for discrepancy can be an effect of external salt concentration on the partitioning coefficient, Φ_i. Indeed, a ~15% decrease in Φ_i when c_f changes from 200 mM to 600 mM, would explain the discrepancy between data and theory, and thus would lead to a much better fit. Thus, a physical or chemical force related to ion entry in the membrane that would make coions not absorb about 9× better when c_f goes up by a factor of 3, as predicted by Eq. (1), but only about 6.5×, would bring the model much closer to the data in all three datasets. Thus, according to this approach, we must identify an additional force that progressively counteracts coion absorption the larger is the salinity of the feedwater. This is a useful line of research, but we followed a different strategy.

RO membranes have a very good exclusion of coions and counterions. However, they also have a quite significant charge density due to the ionizable carboxylic and amine groups. An estimate for the charge density at intermediate pH is that it is of the order of –0.2 M (a negative charge). To attract the counterions in the membrane (cations in this case), a significant negative Donnan potential develops. And when the external salt concentration is lowered, this potential is more negative, to more strongly attract the cations into the membrane. But as a consequence of this Donnan potential, also H^+-ions and OH^--ions respond, and they will absorb or desorb more or less too. Focusing on the H^+-ions, they absorb in the membrane, and the more they do, the more they protonate the carboxylic negative charge, thereby reducing the membrane charge. This effect is larger at a lower salt concentration because then the Donnan potential is more negative, which more strongly attracts the protons into the membrane. Thus, the membrane charge decreases when the salt concentration goes down, as also analyzed in Wang et al. (1997), Chmiel et al. (2006), Yaroshchuk et al. (2019). We can combine a Donnan equation for a 1:1 salt with a Langmuir equation for protonation of acidic groups, which leads to (Yaroshchuk et al., 2019)

$$\begin{aligned} |X| &= 2\Phi_i c_\infty \sinh\left(|\phi_D|\right) \\ |X_{max}|/|X| &= 1 + K\, \exp\left(|\phi_D|\right) \end{aligned} \tag{7}$$

where salt concentration c_∞ refers to a salt concentration just outside the membrane, and ϕ_D is the Donnan potential. The maximum charge density when all membrane groups are ionized is $|X_{max}|$ and K is a factor that depends on pH outside the membrane and pK of the ionizable groups. We set up Eq. (7) for an acidic material, and assume that pH just outside the membrane is not influenced by flow or salt concentration.

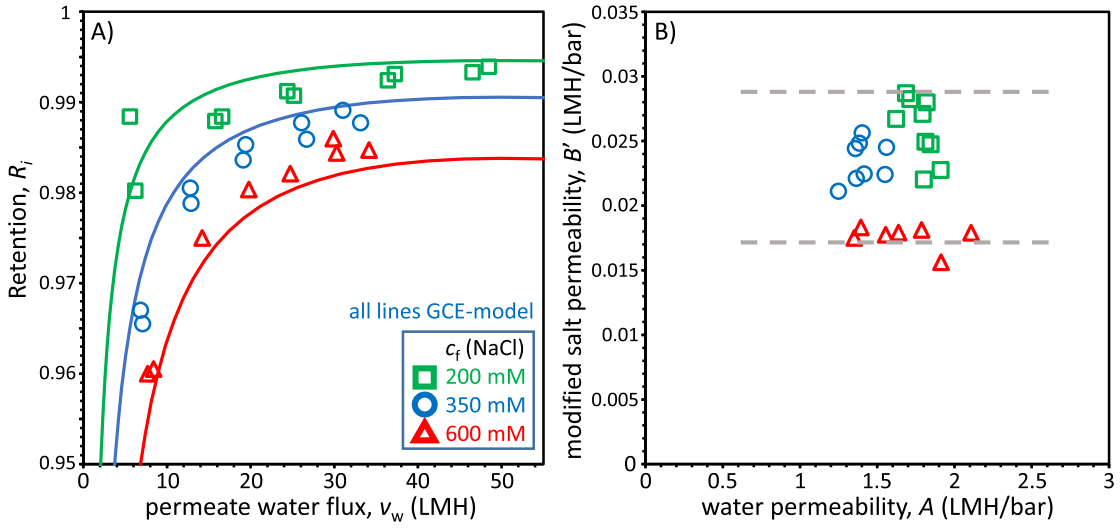

Fig. 2. A) Same data as in Fig. 1 but with 'expanded' y-axis. The GCE-model fits data well, similar to the data fit in Wang et al. (2021). B) In this analysis, the modified salt permeability, B', is not uniquely defined, with almost a factor two difference between lower and upper bounds. Lines in panel A based on fit with $B' = 0.020$ LMH/bar.

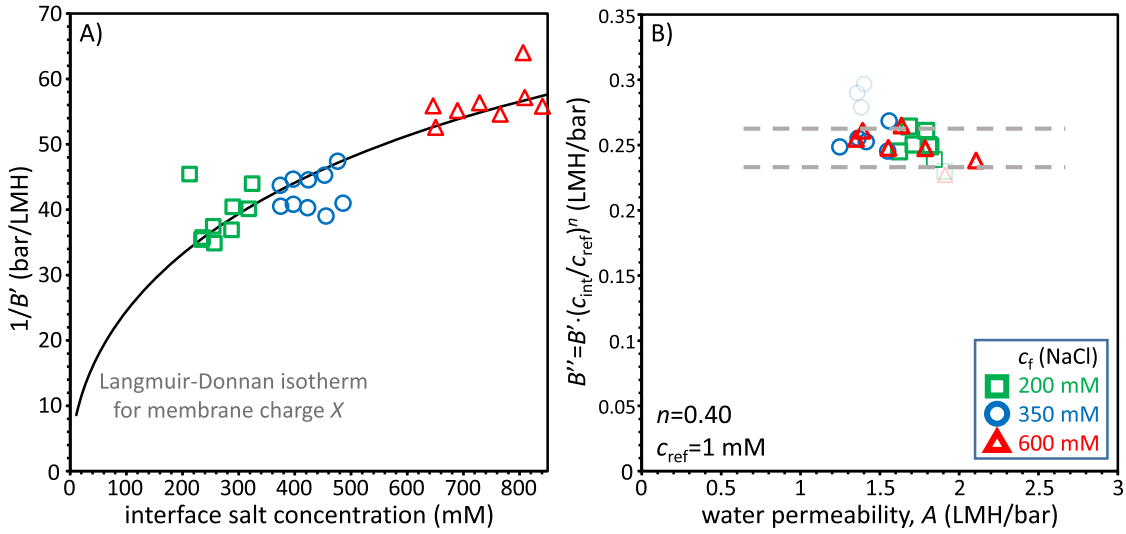

Fig. 3. A) Values of B' from Fig. 2B inverted and plotted versus interface salt concentration, c_{int}. The inverse of B' is proportional to charge density, X, and the continuous line follows from the Langmuir-Donnan model, using an arbitrary multiplier to show the fit. B) Data of the modified salt permeability B'' all converge to a small bandwidth, of $B'' = 0.25 \pm 0.01$ LMH/bar.

Equation (7) describes that the lower is c_∞, the more negative is the Donnan potential, and thus the lower is pH in the membrane and the lower is the membrane charge density, $|X|$, i.e., the closer it is to zero. We make this calculation for the upstream side of the membrane, thus based on c_{int}, and assume that this analysis then holds for the entire membrane. (Alternatively, we do it both for the up- and downstream sides, the latter based on c_p, and then take an average value.)

To analyze this extension of the GCE-model, we present in Fig. 3A the data of B' of Fig. 2B inverted and plotted against the interface concentration, c_{int}. If all parameters that determine B' are independent of salt concentration except for charge density, X, then this dataset of the inverse of B' versus c_{int} must coincide with, must be proportional to, how charge density X depends on c_{int} according to the Langmuir-Donnan (LD) model. And indeed, as Fig. 3A demonstrates, we can easily derive parameter settings for the LD model to arrive at a perfect fit. We can also identify quite well whether certain data points in the dataset are likely outliers, based on a too large deviation from this common trend. In Fig. 3B we have given these points a diminished prominence in the visual presentation. We can use this semi-analytical LD model in the steps that follow, but we prefer to use a simple power law $X \propto c_{int}^{\,n}$, where power n is equal to $n = 0.40$, which fits the LD curve almost perfectly. If we follow this approach, a modified salt permeability is arrived at given by $B'' = B' \cdot (c_{int}/c_{ref})^n$ ($c_{ref} = 1$ mM), and analyzing all data, and extracting for each a value of B'', has the result that all salt permeability data converge to a common value with a narrow distribution, given by $B'' = 0.25 \pm 0.01$ LMH/bar, see Fig. 3B. Though our study does not provide information on the various parameters identified in the definition of B' in Eq. (3), we can nevertheless make a tentative example calculation. If we assume a charge density of $|X| = 200$ mM at a salt concentration of $c_\infty = 500$ mM, and we assume a friction coefficient of $K_{f,i} = 0.04$ and a partition coefficient also of $\Phi_i = 0.04$ (these seem realistic numbers given that both numbers theoretically must be between 0 and 1, and for a functional RO membrane with good ion exclusion and ion friction, we expect numbers rather closer to 0 than to 1), then with the value of B'' just derived, the membrane transport coefficient is $k_{m,i} \sim 0.45$ mm/s, and with an estimate of the membrane thickness of $L_m \sim 100$ nm, the dif-

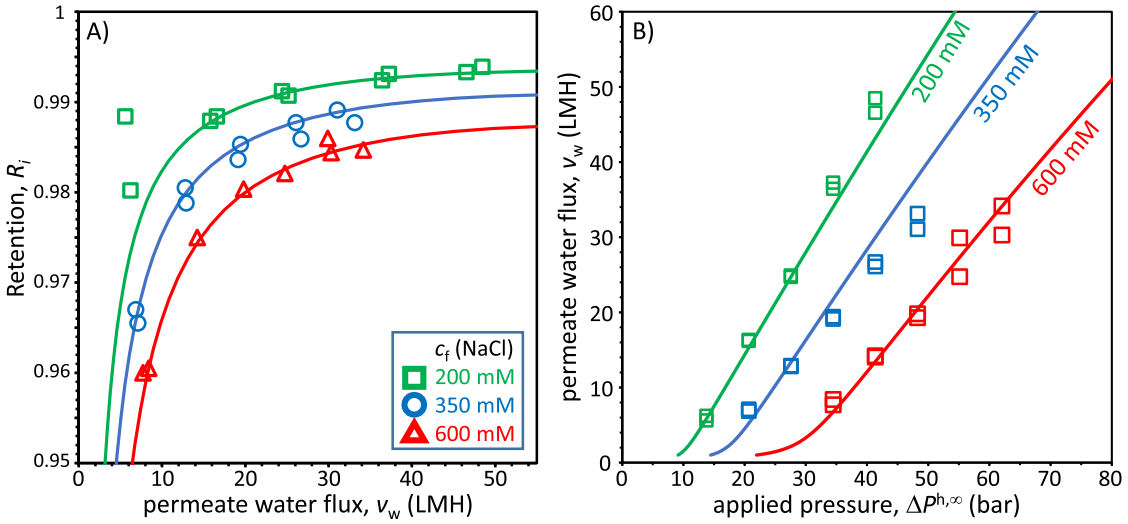

Fig. 4. A) Theory and data for salt retention according to the improved GCE-model with $B''=0.25$ LMH/bar ($n=0.40$), which can be compared with Fig. 2A. B) Theory and data for permeate water flux, v_w, versus applied pressure, $\Delta P^{h,\infty}$, with $A=1.65$ LMH/bar.

fusion coefficient of the ions in the membrane, $D_{m,i}$, is about 40 times lower than in free solution ($k_{m,i} = D_{m,i}/L_m$). All of these numbers seem very reasonable estimates.

Finally we compare this improved GCE-model with the original dataset from Wang et al. (2021) in Fig. 4A, while in Fig. 4B we present results of water flux, v_w, versus pressure, $\Delta P^{h,\infty}$. In Fig. 4A,B we can observe a perfect fit of the improved GCE-theory to the data. This very good fit provides confidence that this theory can be reliably used in studies that aim for improved RO membrane and module analysis, design, and performance optimization.

Let us briefly reiterate how the modified salt permeability B'' was obtained from data, a procedure that can easily be repeated for other datasets. We assume knowledge of salt transport in the CP-layer, resulting for each data point in an estimate of the interface concentration, c_{int}. From the measured permeate concentration, c_p, salt flux is determined by multiplying permeate concentration with the permeate water flux in LMH. This salt flux is then divided by $c_{int}^2 - c_p^2$, and subsequently divided by RT. With concentrations in mM (mol/m^3), this group now has unit LMH/Pa. We multiply by 10^5 to arrive at B' with dimension LMH/bar. We then make the power law correction by multiplying B' with $(c_{int}/c_{ref})^n$ (with $c_{ref}=1$ mM and $n=0.40$). Thus the higher is c_{int}, the higher B'' comes out relative to B'. This parametrization was based on the GCE-model combined with the LD approach to calculate membrane charge, and as Figs. 3 and 4 show, it fits available data perfectly and provides a unique value of B''. Thus this simple model can be reliably used in calculations of modules and systems that use RO to treat a monovalent salt solution. In addition, the parametrization to derive a value of B'' is highly suitable to compare different membranes based on the key membrane properties A and B''. We propose that it is better when diagrams to study the tradeoff between water-salt selectivity and water permeability (Geise et al., 2011; Ritt, 2022) are based on a new selectivity parameter, A/B'' (which is dimensionless, in contrast to the standard A/B-selectivity), plotted versus A. For the tested membrane, we derive a value of $A/B'' \sim 6.6$. To explain the method of data analysis, we provide a simple Excel spreadsheet file as Supplementary Material.

When applying the GCE equations in a theoretical study, for instance of a complete module, the approach to derive a B''-value, is inverted. Now we start with a known input value of the salt permeability B'' (it will depend on salt type and temperature), and B' is calculated at each c_{int} by dividing B'' by $(c_{int}/c_{ref})^n$. This expression for B' (dependent on c_{int}) is then used in the GCE-model, Eq. (2), and that equation can be used in full module-scale simulations.

In conclusion, we demonstrated how the good coion exclusion (GCE) model can be empirically modified to account for a reduction in membrane charge at low salinity, which increases salt permeability. With this effect implemented, a perfect fit of the GCE model to data of water desalination by reverse osmosis was achieved at several values of salt concentration and applied pressure. A unique and discrete (A,B'') point can now be determined for any membrane that operates in this regime. This point does not depend on feed salt concentration or applied pressure. It probably depends on salt type and temperature, and that dependency can now be studied accurately. This unique point can be plotted in permeability-selectivity tradeoff diagrams, and used to reliably compare performance of different RO membranes. With this new parametrization of RO membranes for water desalination, a significant improvement is achieved over the present situation where salt permeability B is not an intrinsic property of a given membrane as it is highly dependent on feed salt concentration.

Declaration of Competing Interest

All authors have participated in (a) conception and design, or analysis and interpretation of the data; (b) drafting the article or revising it critically for important intellectual content; and (c) approval of the final version.

This manuscript has not been submitted to, nor is under review at, another journal or other publishing venue.

The authors have no affiliation with any organization with a direct or indirect financial interest in the subject matter discussed in the manuscript.

Supplementary material

Supplementary material associated with this article can be found, in the online version, at doi:10.1016/j.memlet.2021.100010.

References

A technical note on data analysis: In plots of B vs A, some data at low v_w are left out because either A or B is far off. Data for 600 mM obtained in twofold at a pressure of 42 bar and 48 bar are presented as average because of a large difference between the two points.

Biesheuvel, P.M., 2011. Two-fluid model for the simultaneous flow of colloids and fluids in porous media. J. Colloid Interface Sci. 355, 389–395.

Biesheuvel, P.M., Zhang, L., Gasquet, P., Blankert, B., Elimelech, M., van der Meer, W.G.J., 2020. Ion selectivity in brackish water desalination by reverse osmosis: theory, measurements, and implications. Environ. Sci. Technol. Lett. 7, 42–47.

Bowen, W.R., Welfoot, J.S., 2002. Modelling the performance of membrane nanofiltration–critical assessment and model development. Chem. Eng. Sci. 57, 1121–1137.
Chen, X., Boo, C., Yip, N.Y., 2021. Influence of solute molecular diameter on permeability-selectivity tradeoff of thin-film composite polyamide membranes in aqueous separations. Water Res. 201, 117311.
Chmiel, H., Lefebvre, X., Mavrov, V., Noronha, M., Palmeri, J., 2006. Computer simulation of nanofiltration, membranes and processes. In: Rieth, M., Schommers, W. (Eds.), Handbook of Theoretical and Computational Nanotechnology, Vol. 5. Amer. Sci. Publ., pp. 93–214.
Elimelech, M., Phillip, W.A., 2011. The future of seawater desalination: energy, technology, and the environment. Science 333, 712–717.
Gamaethiralalage, J.G., Singh, K., Sahin, S., Yoon, J., Elimelech, M., Suss, M.E., Liang, P., Biesheuvel, P.M., Zornitta, R.L., de Smet, L.C.P.M., 2021. Recent advances in ion selectivity with capacitive deionization. Energy Env. Sci. 14, 1095–1120.
Geise, G.M., Park, H.B., Sagle, A.C., Freeman, B.D., McGrath, J.E., 2011. Water permeability and water/salt selectivity tradeoff in polymers for desalination. J. Membr. Sci. 369, 130–138.
Kedem, O., Freger, V., 2008. Determination of concentration-dependent transport coefficients in nanofiltration: defining an optimal set of coefficients. J. Membr. Sci. 310, 586–593.
Kedem, O., Katchalsky, A., 1961. A physical interpretation of the phenomenological coefficients of membrane permeability. J. Gen. Physiol. 45, 143–179.
Kimani, E.M., Kemperman, A.J.B., van der Meer, W.G.J., Biesheuvel, P.M., 2021. Multicomponent mass transport modeling of water desalination by reverse osmosis including ion pair formation. J. Chem. Phys. 154, 124501.
Lonsdale, H.K., Merten, U., Riley, R.L., 1965. Transport properties of cellulose acetate osmotic membranes. J. App. Polym. Sci. 9, 1341–1362.
Oren, Y.S., Biesheuvel, P.M., 2018. Theory of ion and water transport in reverse osmosis membranes. Phys. Rev. Appl. 9, 024034.
Riley, R.L., Lonsdale, H.K., Lyons, C.R., 1971. Composite membranes for seawater desalination by reverse osmosis. J. App. Polym. Sci. 15, 1267–1276.
Ritt, C.L., 2022. The open membrane database: synthesis-structure-performance relationships of reverse osmosis membranes. J. Membr. Sci. 641, 119927.
Song, L., 2000. Thermodynamic modeling of solute transport through reverse osmosis membrane. Chem. Eng. Comm. 180, 145–167.
Sonin, A.A., 1976. Osmosis and ion transport in charged porous membranes: a macroscopic, mechanistic model. In: Sélégny, E. (Ed.), Charged Gels and Membranes I. D. Reidel, Dordrecht, pp. 255–265.
Starov, V.M., Churaev, N.V., 1993. Separation of electrolyte solutions by reverse osmosis. Adv. Colloid Interface Sci. 43, 145–167.
Tedesco, M., Hamelers, H.V.M., Biesheuvel, P.M., 2018. Nernst-planck transport theory for (reverse) electrodialysis: III. Optimal membrane thickness for enhanced process performance. J. Membr. Sci. 565, 480–487.
Teorell, T., 1956. Transport phenomena in membranes. eighth Spiers memorial lecture. Discuss. Faraday Soc. 21, 9–26.
Wang, L., Cao, T., Dykstra, J.E., Porada, S., Biesheuvel, P.M., Elimelech, M., 2021. Salt and water transport in reverse osmosis membranes: beyond the solution-diffusion model. Environ. Sci. Technol. 55, 16665–16675. doi:10.1021/acs.est.1c05649.
Wang, X.L., Tsuru, T., Nakao, S.I., Kimura, S., 1997. The electrostatic and steric-hindrance model for the transport of charged solutes through nanofiltration membranes. J. Membr. Sci. 135, 19–32.
Werber, J.R., Osuji, C.O., Elimelech, M., 2016. Materials for next-generation desalination and water purification membranes. Nat. Rev. Mater. 1, 16018.
Wijmans, J.G., Baker, R.W., 1995. The solution-diffusion model: a review. J. Membr. Sci. 107, 1–21.
Wijmans, J.G., Nakao, S., van den Berg, J.W.A., Troelstra, F.R., Smolders, C.A., 1985. Hydrodynamic resistance of concentration polarization boundary layers in ultrafiltration. J. Membr. Sci. 22, 117–135.
Yaroshchuk, A., Bruening, M.L., Zholkovskiy, E., 2019. Modelling nanofiltration of electrolyte solutions. Adv. Colloid Interface Sci. 268, 39–63.